F-4-3

Extended Abstracts of the 2014 International Conference on Solid State Devices and Materials, Tsukuba, 2014, pp698-699

Reduction of Parasitic Resistance in Ge *n*MOSFETs with NiGe/n^+Ge Junctions by Two-step Phosphorus Ion Implantation

Masahiro Koike, Yuuichi Kamimuta, and Tsutomu Tezuka
Green Nanoelectronics Center (GNC), National Institute of Advanced Industrial Science and Technology (AIST)
Present address: *Corporate R&D Center, Toshiba Corporation, 1, Komukai Toshiba-cho, Saiwai-ku, Kawasaki, 212-8582, Japan*
Phone: +81-44-549-2314 Fax: +81-44-520-1257 m-koike@mail.rdc.toshiba.co.jp

Abstract

Two-step P-ion implantation (P-I/I) was investigated as a means to reduce contact resistance (R_C) at metal/n^+Ge junctions. It was clarified that R_C was lower in NiGe/n^+Ge than in Ti/n^+Ge and that the higher formation temperature (≥500°C) of n^+Ge and higher 2nd P-I/I dose (≥1×10^{15} cm^{-2}) resulted in lower R_C. Ge *n*MOSFETs with NiGe/n^+Ge junctions fabricated under the above conditions for low R_C revealed a reduction in parasitic resistance, leading to high I_{ON} while maintaining low I_{OFF}.

1. Introduction

High motilities of electrons and holes in Ge [1] make it a promising alternative to the conventional Si channel material for MOSFETs; however, to realize Ge *n*MOSFETs, the issue of high contact resistance (R_C) of NiGe/*n*Ge must be resolved [2-6].

We previously reported two-step P-ion implantation (P-I/I) as a way to reduce R_C [6]; the 1st P-I/I is used to form n^+/p junctions, i.e., source/drain (S/D) on *p*Ge(100) substrate, and the 2nd P-I/I is used to form the NiGe/n^+Ge interface with a high P concentration.

The two-step P-I/I was found to be effective in reducing the R_C of NiGe/n^+Ge junctions, while maintaining the reverse current level of conventional n^+/p junctions. A possible model is that the P in the 2nd I/I is electrically active around the NiGe/n^+Ge interface, even though the temperature used for germanidation (350°C) was insufficient; however, the dependence of the process parameters on R_C is still unclear. Moreover, the effect of two-step P-I/I on the electrical characteristics of Ge *n*MOSFETs has not been investigated.

In the present study, we examined the R_C of metal/n^+Ge junctions on *p*Ge under various conditions such as different P doses, Ti contact as well as NiGe contact, and different formation temperatures of n^+Ge, using two-step P-I/I. It was revealed that the parasitic resistance (R_{para}) in Ge *n*MOSFETs with NiGe/n^+Ge junctions was reduced by two-step P-I/I under the appropriate conditions, leading to a high I_{ON} while maintaining a low I_{OFF}.

2. Experiment

Ge *n*MOSFETs [Fig. 1(a)] were fabricated as follows: 4-in *p*Ge(100) wafers (0.05–0.25 Ωcm) with SiO_2 isolation were used as substrates. After DHF treatment and O_3 passivation, an Al_2O_3 gate dielectric layer was deposited (~2.5 nm EOT). TaN was deposited as the gate electrode, which was then patterned by EB lithography and RIE process. Implantation of P ions (dose of 1×10^{15} cm^{-2} and acceleration energy of 10 keV) was conducted (1st P-I/I), followed by RTA at 400°C or 500°C in N_2 for 1 min to form n^+Ge S/D regions. After SiO_2 deposition and contact hole formation, additional P ions (0, 2×10^{14}, 1×10^{15}, or 5×10^{15} cm^{-2}, 10 keV) were implanted (2nd P-I/I) into the S/D regions [Fig. 1(b)]. Ni film (10 nm) was deposited on the wafer and annealed at 350°C in N_2 for 1 min to form NiGe (~20 nm)/n^+Ge in the contact hole regions. Then, the wafers were treated with HCl solution to remove unreacted Ni, which was followed by Ti deposition. Similarly to NiGe/n^+Ge, Ti/n^+Ge was also fabricated, where it was annealed at the same temperature as for germanidation before Ti deposition.

3. Results and Discussion

Each of the NiGe/n^+Ge and Ti/n^+Ge junctions revealed a different dependence of the 2nd P-I/I dose on R_C. The *J-V* characteristics of NiGe/n^+Ge junctions based on Kelvin pattern showed an increase in the current with the 2nd P-I/I dose (Fig. 2). The R_C, which was estimated from the *J-V* characteristics, decreased with the increase in the 2nd P-I/I dose, and reached the lowest value at 5×10^{15} cm^{-2} [Fig. 3(a)]. We considered that the 2nd P-I/I increased the electrically active P atoms around the NiGe/n^+Ge interface, reducing the effective Schottky barrier height and the R_C. Ti/n^+Ge junctions also showed that the R_C decreased with the 2nd P-I/I doses of 2×10^{14} and 1×10^{15} cm^{-2}. Our previous work showed an increase in the R_C of Ti/n^+Ge formed by two-step P I/I, probably because annealing was not carried out after the 2nd P-I/I, preventing the recovery of Ti/n^+Ge from I/I damage [Fig. 3(b)] and causing residual defects that deactivated P in n^+Ge. Similarly, the reason why the R_C of Ti/n^+Ge started to increase at the dose of 1×10^{15} cm^{-2} is possibly that the higher 2nd P-I/I dose caused more I/I damage. Although a model of the germanidation in which the P around the NiGe/Ge interface is electrically active has been proposed [7], the results for Ti/n^+Ge suggest that germanidation is unnecessary.

It was revealed that the formation temperature of the n^+Ge layer affected the R_C. NiGe/n^+Ge and Ti/n^+Ge, where n^+Ge layers were formed at lower temperature (400°C), had a higher R_C [Fig. 3(b)]. The R_C of NiGe/n^+Ge where the n^+Ge layer was formed at 600°C in our previous study was lower than that in the present study. This temperature dependence would also be related to the residual defects by the 2nd P-I/I, because a higher temperature can decrease more residual defects in the n^+Ge layer; however, a high temperature causes electrical degradation of the gate stack. Therefore, it is necessary to select the appropriate temperature, which was ≤500°C in our study, taking into account the electrical activation of P in Ge and degradation of the gate stack.

Similarly to R_C, the sheet resistance (R_S) of n^+Ge was estimated from the *J-V* characteristics of NiGe/n^+Ge/NiGe based on Kelvin pattern (Fig. 4). R_S remained unchanged for the 2nd P-I/I dose (Fig. 5), which is reasonable given that it was determined by the n^+Ge region without the 2nd P I/I. On the other hand, R_S was lower in the n^+Ge layer formed at 500°C than at 400°C, which would be similarly related to the residual defects described above.

We confirmed that the reverse current level of n^+/p junctions was maintained irrespective of the 2nd P-I/I (Fig. 6). This suggests that the 2nd P-I/I did not generate a defect-related leakage current. On the other hand, the ratio of J_F at –1 V to J_R at 1 V in the *J-V* characteristics amounted to ~10^7. Note that J_F increased with the 2nd-P I/I dose, suggesting the reduction of R_C.

Ge *n*MOSFETs with NiGe/n^+Ge junctions formed by two-step P-I/I revealed an increase in I_D. I_D-V_G characteristics of the device [Fig. 7(a)] showed that I_D increased in the 2nd P-I/I dose, and reached almost the same level as that at the dose of ≥1×10^{15} cm^{-2}. On the other hand, the subthreshold slope remained almost the same for the devices irrespective of the 2nd P-I/I [Fig. 7(b)].

The increase in I_D originated from the reduction of R_{para}, which was estimated based on the relationship between the gate length (L_G) and the total resistance (R_{total}) and by the effective channel length method [8]. The R_{total} at which the fitted lines converge corresponds to the R_{para} (Fig. 8). The R_{para} decreased with increasing 2nd P-I/I dose [Fig. 9(a)].

The R_{para} was reduced due to the reduction of R_C. The R_{para} for Ge *n*MOSFETs in the present study is summarized in Fig. 9(a); for instance, in the case of NiGe/n^+Ge junctions with the n^+Ge layer formed at 500°C, R_{para} decreased with increasing 2nd P-I/I dose. We confirmed that R_{para} corresponded to the sum of 2R_C and 2R_S [Fig. 9(b)], where R_S of the n^+Ge region between the gate edge and contact hole (Fig. 1) was estimated from R_S based on Kelvin pattern (Fig. 5). In the case without the 2nd P-I/I, 2R_C was dominant in the R_{para}. With increasing 2nd P-I/I dose, 2R_C decreased to ~180 Ωμm, resulting in the lowest R_{para} of ~470 Ωμm.

Thus, two-step P-I/I can reduce the R_{para} because of the reduction of R_C, leading to the increase of I_{ON} in Ge *n*MOSFETs.

4. Summary

Two-step P-I/I was investigated as a means to reduce the R_C of metal/n^+Ge junctions. It was clarified that R_C was lower in NiGe/n^+Ge than in Ti/n^+Ge and that the higher formation temperature (≥500°C) of n^+Ge and higher 2nd P-I/I dose (≥1×10^{15} cm^{-2}) resulted in lower R_C of NiGe/n^+Ge. Since the two-step P-I/I resulted in negligible R_C compared with R_{para}, Ge *n*MOSFETs (L_G: 110–350 nm) fabricated under the above conditions for low R_C could enhance I_{ON} while maintaining low I_{OFF}. Thus, two-step P-I/I is effective for fabricating Ge *n*MOSFETs with a high I_{ON} and a low junction leakage current.

Acknowledgments

We would like to thank all the technical staff of AIST for supporting our experiment. This research was supported by a grant from JSPS through the FIRST Program initiated by CSTP.

References

[1] S. M. Sze, Physics of Semiconductor Devices (Wiley, New York, 1981) 2nd ed.
[2] A. Dimoulas *et al*., Appl. Phys. Lett. **89**, 252110 (2006).
[3] P. Tsipas and A. Dimoulas, Appl. Phys. Lett. **94**, 012114 (2009).
[4] M. Koike *et al*., Appl. Phys. Express **4,** 021301 (2011).
[5] M. Koike *et al*., Appl. Phys. Lett. **102,** 032108 (2013).
[6] M. Koike *et al*., Appl. Phys. Express **7**, 051302 (2014).
[7] T. Nishimura *et al*., Appl. Phys. Express **2**, 021202 (2009).
[8] K. Terada and H. Muta, Jpn. J. Appl. Phys. **18**, 953 (1979).

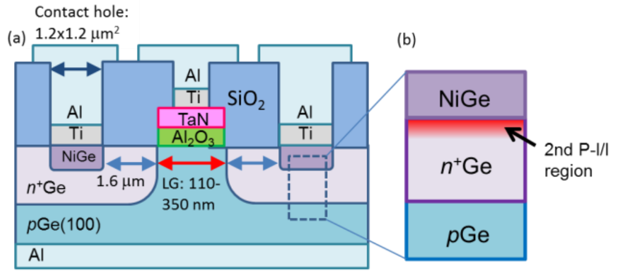

FIG. 1: (a) Structure of Ge *n*MOSFET fabricated in the present study, and (b) enlarged view of NiGe/n^+Ge with 2nd P-I/I region.

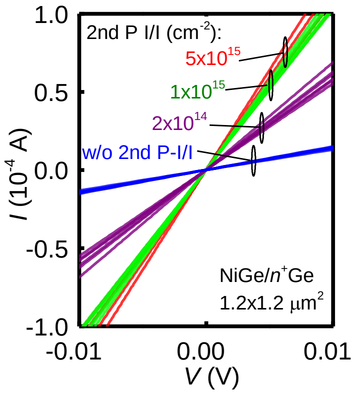

FIG. 2: *J-V* characteristics of Ni-Ge/n^+Ge based on Kelvin pattern, where n^+Ge was formed at 500°C. The 2nd P-I/I doses were 0, 2×10^{14}, 1×10^{15}, and 5×10^{15} cm^{-2}.

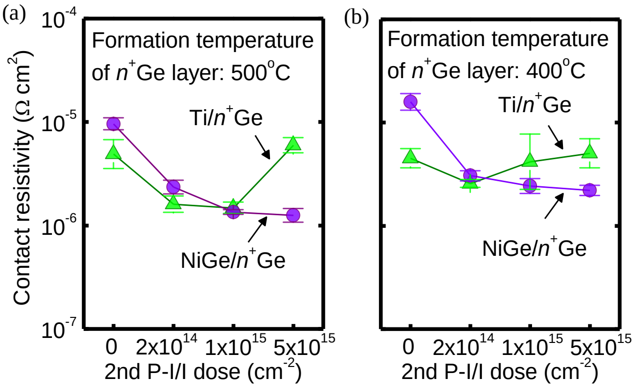

FIG. 3: Dependence of 2nd P-I/I dose on R_C of NiGe/n^+Ge junctions. R_C was estimated from *J-V* characteristics in Fig. 2. The n^+Ge layers were formed at (a) 500°C and (b) 400°C. Contact hole size was 1.2×1.2 μm^2, the same as that in Ge *n*MOSFETs (Fig. 1). Error bar shows the 95% confidence interval of the lognormal distribution.

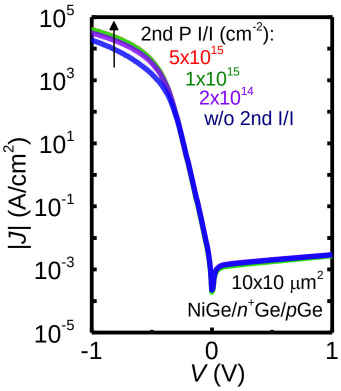

FIG. 6: *J-V* characteristics of NiGe/n^+Ge/*p*Ge(100) junctions formed by two-step P-I/I, where n^+Ge was formed at 500°C.

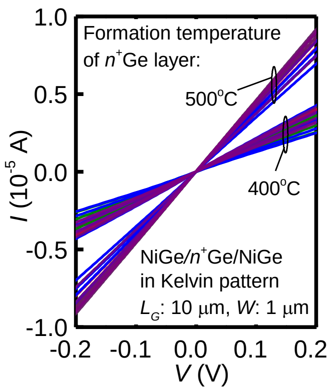

FIG. 4: *J-V* characteristics of Ni-Ge/n^+Ge/NiGe formed by two-step P-I/I in Kelvin pattern for R_S estimation.

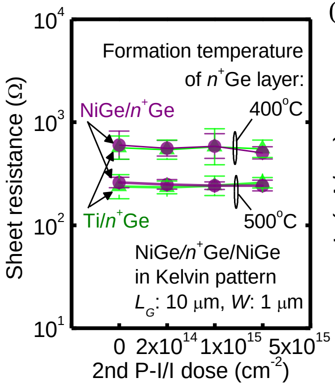

FIG. 5: Dependence of 2nd P-I/I dose and formation temperature of n^+Ge on R_S, which was estimated from *J-V* characteristics (Fig 4).

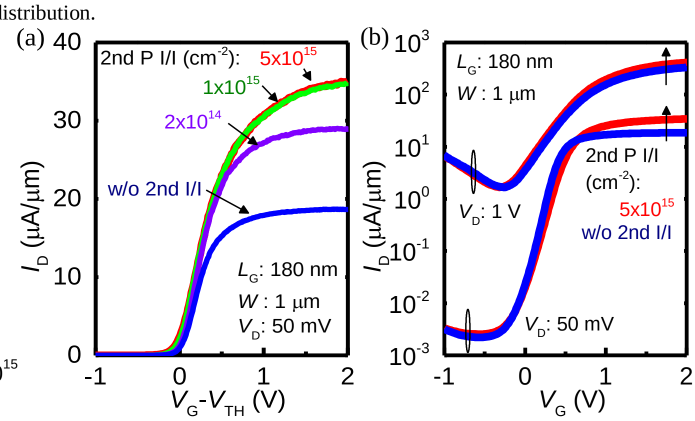

FIG. 7: I_D-V_G characteristics of Ge *n*MOSFETs with NiGe/n^+Ge junctions formed by two-step P-I/I, where n^+Ge was formed at 500°C. (a) Linear plots and (b) log plots.

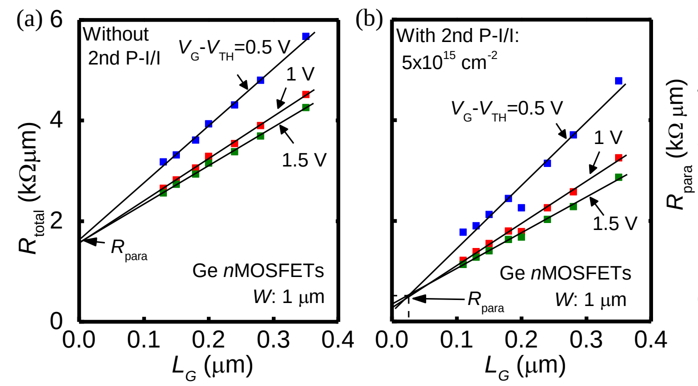

FIG. 8: Relationship between L_G and R_{total} of Ge *n*MOSFETs with NiGe/n^+Ge junctions formed by two-step P-I/I. R_{para} was estimated by the effective channel length method; the values at which the fitted lines converge correspond to R_{para}.

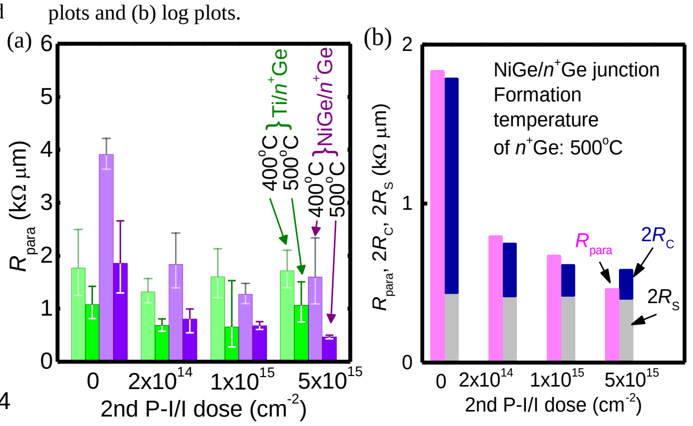

FIG. 9: (a) Summary of R_{para} for MOSFETs in this study, and (b) dependence of 2nd P-I/I dose on R_{para}, R_C and R_S. R_{para} (Fig. 8) was estimated from the L_G-R_{total} relationship of Ge *n*MOSFETs, whereas R_C (Fig. 3) and R_S (Fig. 5) were estimated by Kelvin pattern, respectively.